The blackout of September 2019 on the island of Tenerife: an opportunity to estimate the level of contamination of electromagnetic noise using the magnetotelluric method

EGU General Assembly 2020

David Martínez van Dorth[1] (dmartinez@iter.es), Luca D'Auria[1 2], Juanjo Ledo Fernández[1 3], Perla Piña-Varas[3], Federico Di Paolo[1], Iván Cabrera-Pérez[1], Germán Cervigón[1], Monika Przeor[1], William Hernández[1], Pilar Queralt[3], Alex Marcuello[3], Nemesio M. Pérez[1 2 4]

[1]Instituto Volcanológico de Canarias (INVOLCAN), San Cristóbal de La Laguna, Spain,
[2]Instituto Tecnológico y de Energías Renovables (ITER), Granadilla de Abona, Spain,
[3]GEOMODELS Research Institute, Departament de Dinàmica de la Terra i de l'Oceà, Facultat de Ciències de la Terra, Universitat de Barcelona, Barcelona, Spain,
[4]Agencia Insular de la Energía de Tenerife (AIET), Granadilla de Abona, Spain

1. Introduction

On 29 September 2019, at 13:11:38 (local time) a blackout occurred in the volcanic island of Tenerife (Canary Islands) (Fig. 1). The island electric power system was suddenly shut down in an overpopulated area, representing an interesting opportunity to measure the natural electromagnetic field free of anthropogenic noise. As part of a volcano monitoring project that INVOLCAN is currently performing in the center of the island, a magnetotelluric (MT) station was recording continuously during this event. Therefore, the acquired data allows us to compare the electromagnetic field before and during the blackout.

MT is a passive geophysical method that measures the natural variations of the electromagnetic field to infer the geoelectrical structure of the subsurface. Thus, the five components (Ex, Ey, Hx, Hy and Hz) of the electromagnetic field were recorded with a broadband MT (10^{-3} to 10^{3} s)

The goal of the present work is to show the preliminary results of the evaluation of the effect of the blackout on the measured electromagnetic signals, especially in the frequency range of 256-0.05 Hz.

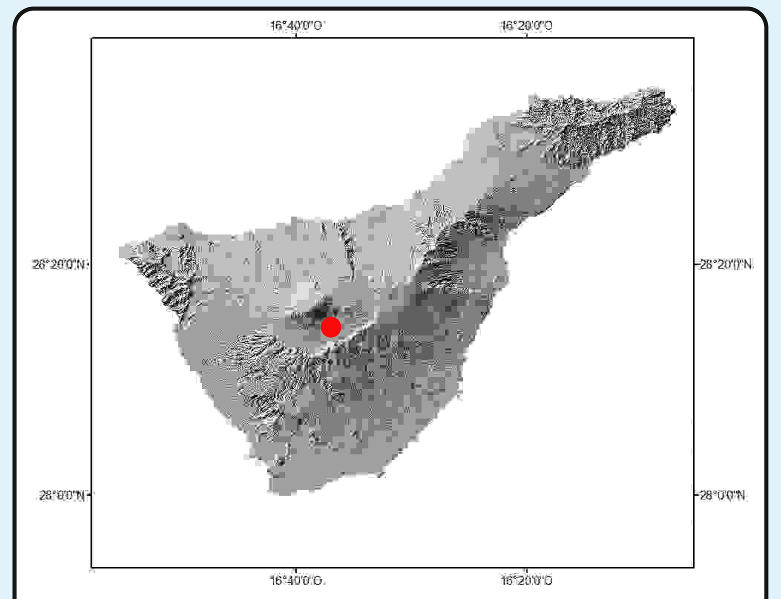

Figure 1. Location of the magnetotelluric site affected by the blackout.

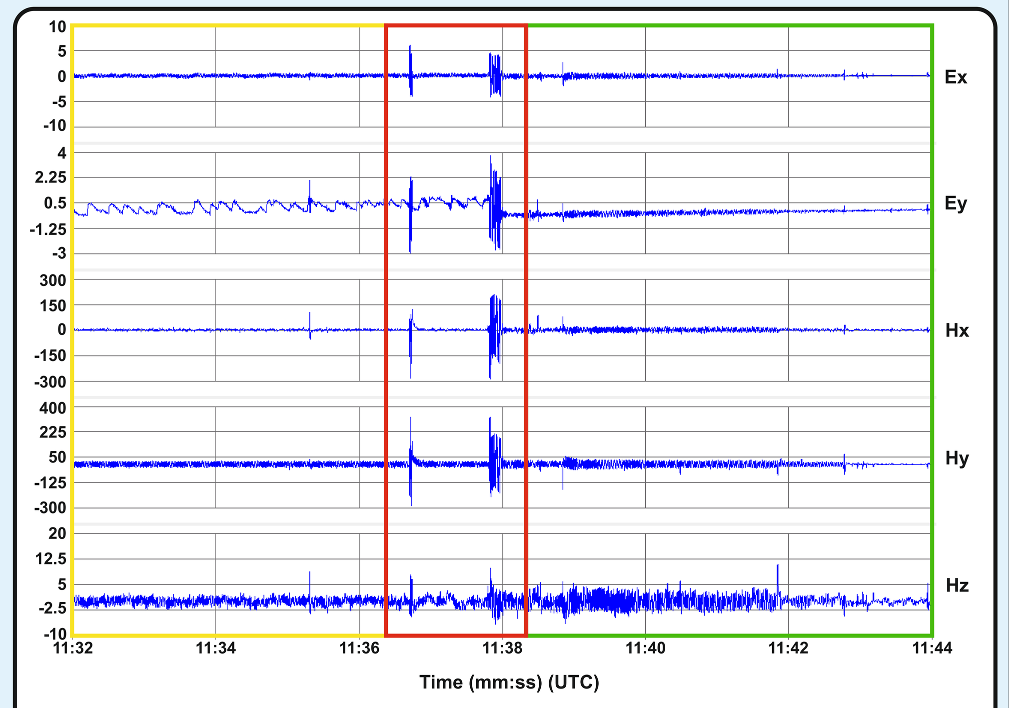

Figure 2. Time series of the electric and magnetic components for a sampling rate of 256 Hz in the beginning of the blackout. On the left side, the scale in milivolts for each component. On the right side, two electric (Ex and Ey) and three magnetic (Hx, Hy and Hz) components. The rectangular shapes mean: 1) Yellow, before the blackout; 2) Red, transients at the onset of the blackout; 3) Green, during the blackout.

2. Spectrogram

The spectrogram reveals the temporal evolution of the frequency content of the signal energy. Only the four horizontal components (Ex, Ey, Hx and Hy) are shown because the event was better reflected in their time series.

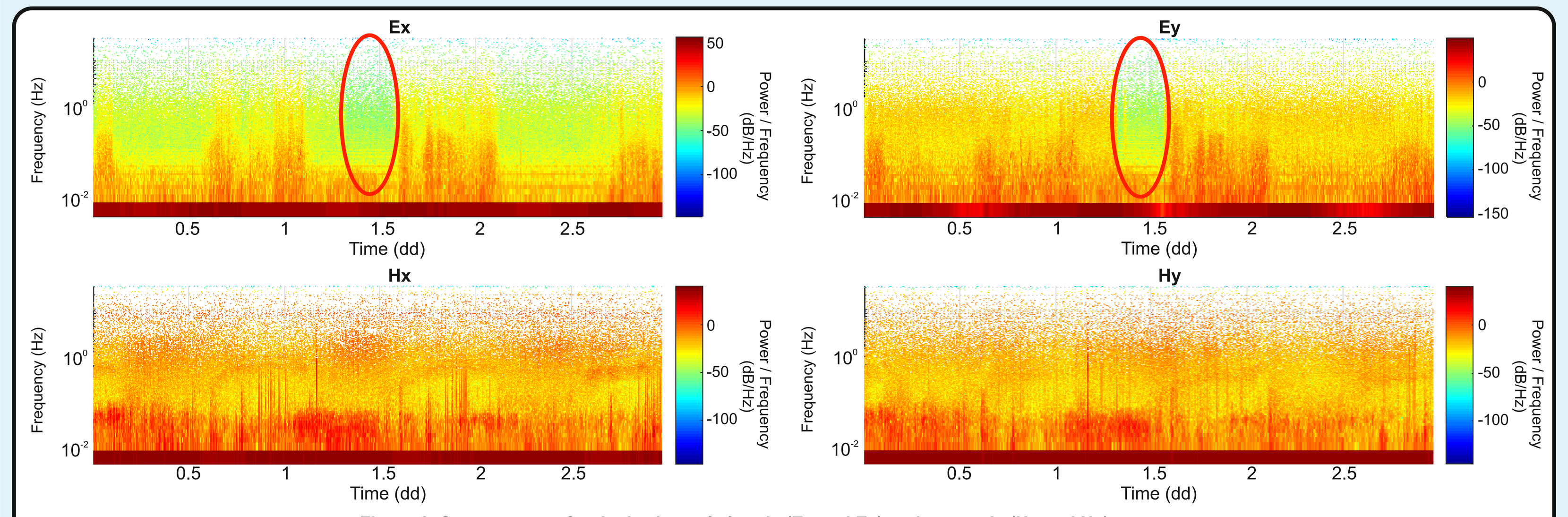

Figure 3. Spectrograms for the horizontal electric (Ex and Ey) and magnetic (Hx and Hy) components.

Figure 3 shows the spectrograms for a sample frequency of 64 Hz and for a total of 3 days. The absence of electromagnetic noise is especially visible on the E-W electric component (Ey), where there is a clear decrease of the power during the blackout.

3. Analysis of the polarization angle

In order to study in detail the behaviour of the electromagnetic signal we applied the wavelet analysis developed by Escalas et al., (2013). In this work the polarization angle is defined as the angle formed with the semi-major axis with the EW direction using an ellipse which helps to determine the direction of the data polarity.

Electric field: In figure 4A there is a remarkable polarized signal for 50 Hz with a polarization angle of 85º that remains constant for the entire spectra, while for most of the recording there is a clear polarization angle of ≈ 14º for the range of 1-32 Hz. In figure 4B the blackout strikes are recorded in the electric field as a signal with a random polarity, which is the expected for natural electromagnetic variations. There are three principle polarization angles: one peak at 141º (> 10 Hz), and two peaks at ≈ 50º and 14º (both < 10 Hz). It seems that around 13.00 h some sort of electromagnetic noise source was temporarily activated in the area, affecting the lower frequencies. In figure 4C the electric system began to recover slowly and the signal of 50 Hz starts to appear varying its polarization angle. Furthermore, the polarization angles of 141º and ≈ 50º also vary but slightly.

I

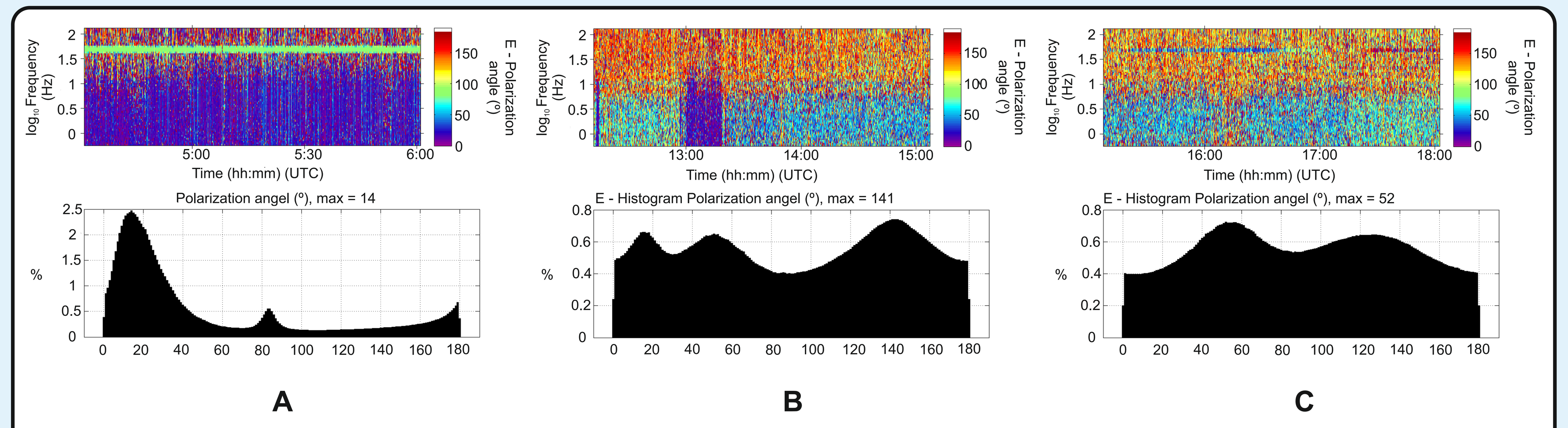

Figure 4. Polarization angle spectrograms and their respective histograms for a sampling rate of 64 Hz: A) Graphics of the previous hours before the blackout; B) Graphics of the beginning of the blackout; and C) Graphics during the blackout.

Magnetic field: in figure 5A there is a polarized signal that extends the entire interval at a frequency of 50 Hz, identical to the one mentioned above, but with a polarization angle of 172º. There is also a large peak for the range 1-10 Hz with a polarization angle of 60-70º. However, in figure 5B during the blackout the signal linearly polarized for 50 Hz with an angle of 172º disappears. The peak located at first in the range of 1-10 Hz focuses now on a peak with a polarization angle of 62º for frequencies > 1 Hz. Finally, in figure 5C the large peak previously mentioned varies smoothly to a peak with a polarization angle of 42º for most of the represented frequency range. Like in the electric field, the signal at 50 Hz starts to appear with a varying polarization angle.

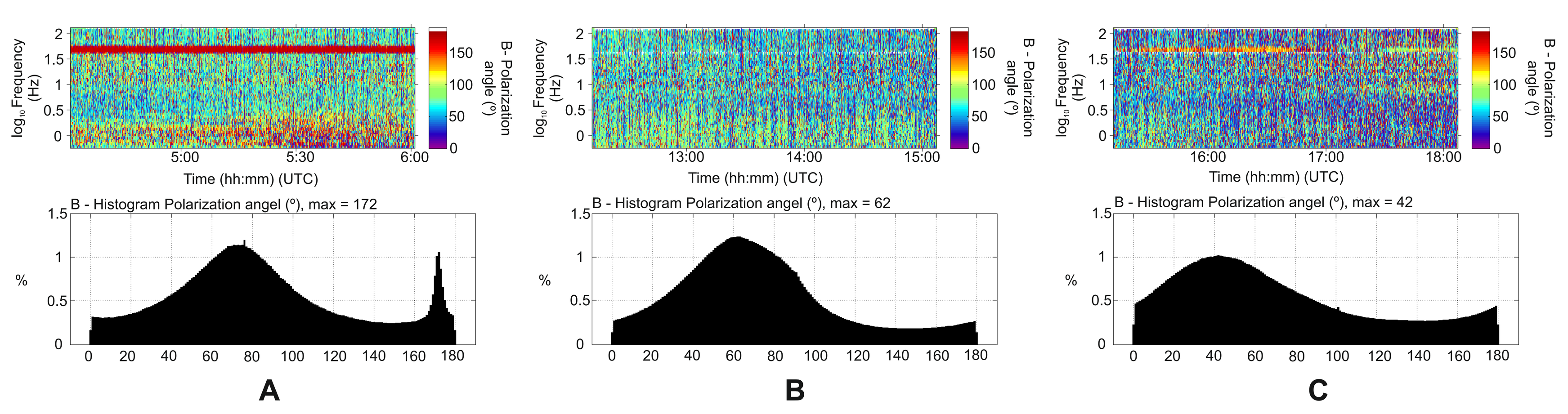

Figure 5. Polarization angle spectrograms and their respective histograms for a sampling rate of 64 Hz: A) Graphics of the previous hours before the blackout; B) Graphics of the beginning of the blackout; and C) Graphics during the blackout.

4. Phase tensor

The Phase Tensor is a technique used to evaluate the dimensionality and the geoelectrical direction of the MT data (Caldwell et al., 2004). Figure 6 shows the phase tensor at different time windows computed with the MTpy (Krieger and Peacock, 2014).

The mid range of frequencies (≈ 10 Hz to 6-7 s) reveals a linear shape until it reaches the blackout. This means that the electric field is linearly polarized.

There is a sharp change on the phase tensor behavior during the blackout time window (12:00 to 18:00 h; Fig. 6). This points out the effect of the electromagnetic noise on the MT data analysis, such as a possible misinterpretation of the geoelectrical dimensionality.

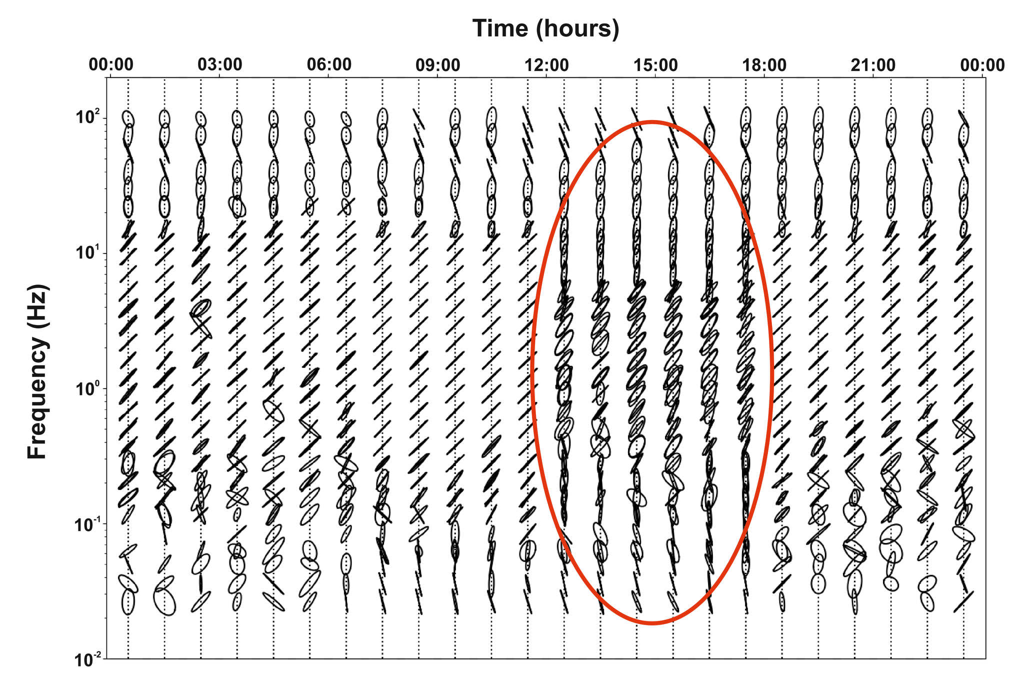

Figure 6. Temporal evolution of the phase tensor for different frequencies.

6. Conclusions

The preliminary analysis performed have demostrated that the magnetotelluric site measured in Las Cañadas Caldera (Tenerife) it is clearly affected by anthropogenic noise at frequencies lower than 50 Hz.

The effect of the blackout on the electromagnetic field is clearly identifiable on the signal, as shown by the previous spectrograms. Moreover, the analysis reveals a clear polarization angle of the electromagnetic signal before the blackout, providing information about the source of noise. Finally, the phase tensor shows that the true geoelectrical dimensionality could be hidden by the electromagnetic noise.

The results obtained in this first stage of the study shows that the data acquired during the blackout could provide valuable information about the effect of the electromagnetic noise in the MT responses. Future woks will be focused on performing a deeper analysis of the signal in order to try to better quantifying the anthropic noise.

References

Escalas, M., Queralt, P., Ledo, J., & Marcuello, A. (2013). Polarisation analysis of magnetotelluric time series using a wavelet-based scheme: a method for detection and characterisation of cultural noise sources. Physics of the Earth and Planetary Interiors, 218, 31-50.

Caldwell, T. G., Bibby, H. M., & Brown, C. (2004). The magnetotelluric phase tensor. Geophysical Journal International, 158(2), 457-469.

Krieger, L., & Peacock, J. R. (2014). MTpy: A Python toolbox for magnetotellurics. Computers & geosciences, 72, 167-175.

Acknowledgements

This research was financially supported by the projects:TFvolcano, financed by Cabildo Insular de Tenerife VOLRISKMAC (MAC/3.5b/124) and VOLRISKMAC II (MAC2/3.5b/328) financed by the Program EU Interreg MAC